

Learning Sequence Descriptor based on Spatio-Temporal Attention for Visual Place Recognition

Fenglin Zhang¹, Junqiao Zhao^{*,1,2}, Yingfeng Cai¹, Gengxuan Tian¹, Wenjie Mu¹, Chen Ye¹

Abstract—Visual Place Recognition (VPR) aims to retrieve frames from a geotagged database that are located at the same place as the query frame. To improve the robustness of VPR in perceptually aliasing scenarios, sequence-based VPR methods are proposed. These methods are either based on matching between frame sequences or extracting sequence descriptors for direct retrieval. However, the former is usually based on the assumption of constant velocity, which is difficult to hold in practice, and is computationally expensive and subject to sequence length. Although the latter overcomes these problems, existing sequence descriptors are constructed by aggregating features of multiple frames only, without interaction on temporal information, and thus cannot obtain descriptors with spatio-temporal discrimination. In this paper, we propose a sequence descriptor that effectively incorporates spatio-temporal information. Specifically, spatial attention within the same frame is utilized to learn spatial feature patterns, while attention in corresponding local regions of different frames is utilized to learn the persistence or change of features over time. We use a sliding window to control the temporal range of attention and use relative position encoding to construct sequential relationships between different features. This allows our descriptors to capture the intrinsic dynamics in a sequence of frames. Comprehensive experiments on challenging benchmark datasets show that the proposed approach outperforms recent state-of-the-art methods. The code is available at <https://github.com/tiev-tongji/Spatio-Temporal-SeqVPR>.

I. INTRODUCTION

Visual place recognition (VPR) aims to retrieve frames from a geo-tagged database that are located at the same place as the queried frame [1]. It is typically used for loop detection in simultaneous localization and mapping (SLAM) as well as for visual relocalization. Various approaches have been proposed to enhance the performance of VPR by learning improved frame representation [2], [3], [4], [5], [6], [7]. However, single frame-based VPR is still susceptible to drastic changes in viewpoint and appearance, so studies have delved into the utilization of sequence information to tackle this issue.

One category of sequence-based methods is based on sequence matching. This approach involves comparing each frame within the query sequence to a set of geo-tagged frames, leading to the creation of a matching matrix. Then, the diagonal values are aggregated to obtain a similarity score

to determine the location of the query sequence. However, this method is mainly suitable for cases where the camera motion remains relatively stable [8]. Otherwise, incorrect matches may occur. Additionally, the computational cost of sequence matching increases with the sequence length and map size [9].

To tackle the challenges mentioned above, researchers have proposed utilizing descriptors to represent a sequence [10]. Sequence descriptors provide better scalability for various sequence lengths and greater robustness against perceptual aliasing caused by using single frame descriptors. However, existing researches only aggregate descriptors [11] or local features of multiple frames [12]. The cross-frame temporal interactions are ignored, which makes sequence descriptors less discriminative.

In this paper, we propose an approach to explore spatio-temporal interactions within frame sequences to extract sequence descriptors. Such sequence descriptors take into account both the temporal correlation across multiple frames and the spatial structure distribution in a frame. Utilizing the attention mechanism, we weight image patches adaptively to capture and combine discriminative features in the sequence. A sliding window is used to control the attentional range and reduce the computational burden. Moreover, relative position encoding is employed to guide the sequence descriptors to learn spatio-temporal patterns rather than the specific visual content. This choice stems from the observation that, during camera motion, the visual content moves with the frame, while the relative positions of spatio-temporal patterns remain constant.

The contributions of this paper are threefold:

- We introduce a spatio-temporal sequence descriptors that effectively captures interaction of the spatial and temporal information simultaneously.
- We investigate the impact of position encoding on spatial and temporal information interactions.
- Our approach delivers competitive results across multiple datasets, outperforming existing state-of-the-art methods based on sequence descriptors.

II. RELATED WORKS

A. Sequence-based VPR

There are mainly two avenues for utilizing sequence information in VPR: sequence matching and sequence descriptors extraction [1].

The sequence matching comprises two key steps. Initially, a similarity matrix is constructed by comparing the

This work is supported by the National Key Research and Development Program of China (No. 2021YFB2501104). (Corresponding Author: Junqiao Zhao.)

¹All authors are with Department of Computer Science and Technology, School of Electronics and Information Engineering, Tongji University, Shanghai, China, and the MOE Key Lab of Embedded System and Service Computing, Tongji University, Shanghai, China (Corresponding Author: zhaojunqiao@tongji.edu.cn)

²Institute of Intelligent Vehicles, Tongji University, Shanghai, China

descriptors of each frame in the query sequence with the descriptors of all frames in the database. Subsequently, the most similar sequence in the database is determined by aggregating the individual similarity scores. SeqSLAM [8] is a pioneering example of sequence matching. However, SeqSLAM can be computationally demanding especially when handling large maps. Additionally, it relies on the assumption of constant velocity, which can limit its applicability in scenarios with varying motion characteristics. To address these challenges, several innovations have emerged. Fast-SeqSLAM [9] leverages an approximate nearest neighbor algorithm to reduce time complexity without degrading the accuracy. [13] proposes a local matching method based on an improved dynamic time warping algorithm, which relaxes the assumption of constant velocity and concurrently reduces time complexity. Nevertheless, these methods may still face the issue of potential mismatches between sequences from different places, due to the presence of several highly similar frames in them.

In the second avenue, a descriptor is extracted to represent a sequence, followed by a direct sequence-to-sequence similarity search. This not only reduces the cost of matching but also incorporates temporal cues into the descriptor. [10] is the first to propose the idea of fusing multiple individual descriptors to generate a sequence descriptor. Subsequently, SeqNet [11] proposes to use a 1-D convolution to perform the learning of frame-level features into a sequence descriptor. However, this approach is implemented based on pre-computed individual frame descriptors, which prevents the sequence descriptors from capturing the local features within each frame. SeqVLAD [12] proposes a detailed taxonomy of techniques using sequence descriptors. It analyzes various mechanisms for fusing individual frame information, and further investigates the feasibility of using the Transformer as the backbone. The sequence descriptor is aggregated by NetVLAD [6] directly from the local features of each frame in the sequence. However, the temporal information interaction across frames is not considered, so they cannot obtain descriptors with spatio-temporal discrimination.

B. Spatio-temporal Attention Mechanism

Spatio-temporal attention mechanisms have found application in various tasks, including video retrieval, video classification, and more. In the context of video action recognition, [14] presents a general ConvNet architecture that leverages multiplicative interactions of spatio-temporal features to capture long-term dependencies among local features. [15] proposes a spatio-temporal attention network to learn the discriminative feature representation for actions. For the video classification task, [16] explores the efficacy of spatio-temporal attention mechanism for feature learning directly from image patches, circumventing the need for spatial or temporal convolutional layers. [17] introduces a novel multi-scale vision transformer, achieving state-of-the-art performance. The spatio-temporal attention mechanism extends its influence to diverse tasks such as image captioning [18] and person re-identification [19].

These methods leverage both spatial and temporal information to selectively focus on pertinent video regions or frames. Interestingly, despite their success in various applications, such techniques have not yet been integrated into sequence-based VPR.

III. METHODOLOGY

We begin by presenting the architecture, which encompasses the spatio-temporal-based feature learning and aggregation. Subsequently, we introduce the loss function.

A. Architecture

The architecture of our model is illustrated in Figure 1. It takes a frame sequence $S \in \mathbb{R}^{L \times H \times W \times 3}$ as input, composed of L image frames, each with dimensions $H \times W$. Since vision transformer [20] is computation-intensive and lacks the inductive biases inherent in convolutional neural networks (CNN) [21], we utilize convolution layers to map each frame s_i to a feature map $m_i \in \mathbb{R}^{h \times w \times c}$, where $s_i \in S$, $i \in \{1, 2, \dots, L\}$ and c represents the number of channels. Subsequently, the feature map of each frame is split into N non-overlapping patches, where N is determined as hw/P^2 , given the patch size of $P \times P$. Following this, each patch is flattened and mapped to an embedding x using a trainable linear projection E .

$$x_{j,patch}^i = E(p_j^i), x_j^i \in \mathbb{R}^D \quad (1)$$

where $i \in \{1, 2, \dots, L\}$, $j \in \{1, 2, \dots, N\}$, and $p \in R^{P \times P}$ which indicates the patch. Then, x is employed as the input embedding for Spatial and Temporal Transformer Encoders.

1) *Spatial Attention*: In each frame, the positions of the local features reflect the spatial distribution of the features, and this distribution remains relatively consistent within a frame under the same view. Similar to ViT [20], we incorporate position information into the patch embedding¹ using a standard learnable absolute position embedding denoted as $x_{pos} \in \mathbb{R}^D$, as illustrated in Figure 2 (a).

$$x_j = x_{j,patch} + x_{j,pos}, x_j \in \mathbb{R}^D \quad (2)$$

We employ an L_s -layer transformer encoder for spatial fusion, which outputs spatial fusion embeddings $\{x_{1,...,N}^{s1}, \dots, x_{1,...,N}^{sL}\}$. Each layer consists of a multi-head self-attention (MSA) module, a multi-layer perceptron (MLP), Layer-norm (LN) blocks and residual connections. In the MSA module, linear projections $W_Q^h, W_K^h, W_V^h \in \mathbb{R}^{d \times D}$ are applied to query (Q^h), key (K^h) and value (V^h) according to Equation 3, where $X = \{x_1, x_2, \dots, x_N\}$, h represents the head index and $d = D/h$. Subsequently, the self-attention weights are computed through the dot-product of Q^h and K^h , then the output $Z^h \in \mathbb{R}^{N \times d}$ is generated by multiplying scaled weights and V^h in Equation 4. Finally, the output $\{Z^1, Z^2, \dots, Z^h\}$ from the heads are concatenated to form $Z \in \mathbb{R}^{N \times D}$ as shown in Equation 5, which serves as input to the Layer-norm and MLP components.

¹The superscript is omitted where it does not cause ambiguity.

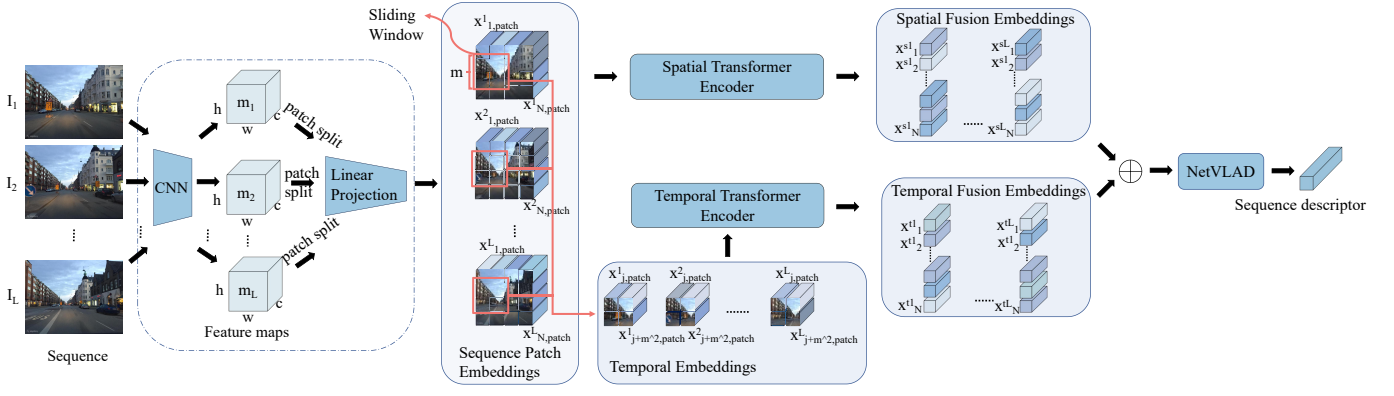


Fig. 1. **The architecture of our proposed method.** Given a continuous sequence of raw frames I_1, I_2, \dots, I_L , we employ a Convolutional Neural Network (CNN) to map each frame to feature maps and then split these maps into patches. A Linear Projection is subsequently employed to map the patch features to embeddings $\{x_{1,\dots,N}^1, x_{1,\dots,N}^2, \dots, x_{1,\dots,N}^L\}$. These embeddings from individual frames are then passed through Spatial Transformer Encoders, applying self-attention for spatial information interaction. This process yields a set of transformed embeddings $\{x_{1,\dots,N}^{s1}, \dots, x_{1,\dots,N}^{sL}\}$. Furthermore, the embeddings across different frames within the sliding window are input into a Temporal Transformer Encoder to fuse temporal information, which generates $\{x_{1,\dots,N}^{t1}, \dots, x_{1,\dots,N}^{tL}\}$. Finally, the embeddings from two branches are combined, and the NetVLAD layer is employed to aggregate these tokens to generate a sequence descriptor.

$$Q^h = W_Q^h X, K^h = W_K^h X, V^h = W_V^h X \quad (3)$$

$$Z^h = \text{Softmax}(Q^h K^{hT} / \sqrt{d}) V^h \quad (4)$$

$$Z = \text{Concat}(Z^1, Z^2, \dots, Z^h) \quad (5)$$

2) *Temporal Attention:* We define a sliding window of size $m \times m$ to control the temporal self-attention range in the sequence. In each layer of temporal transformer attention, self-attention occurs within identical sliding windows of the same region across multiple images. The window moves along the rows and columns, indicating that attention is performed between temporally adjacent regions, as illustrated in Figure 2 (d), rather than between two images.

In temporal interaction, $x_{j,patch}$ from Equation 1 is taken as the input. We redefine X in Equation 3 as $X = \{x_j^1, \dots, x_{j+m^2}^1, \dots, x_j^L, \dots, x_{j+m^2}^L\}$, where L is the frame index, j is the patch index and m is the sliding window size, and generate Q, K, V respectively. We argue that the relative position provides a more accurate description of the consistency or variation of the local features of a sequence over time compared to the absolute position. This is because relative position information can capture the changing relationship between the positions of two patches across different frames, as illustrated in Figure 2 (d), whereas absolute position information merely considers the static relationship of one patch to all patches, as illustrated in Figure 2 (b).

We encode the relative position between two input embeddings x_i and x_j in X , into a relative positional embedding $P_{ij} \in \mathbb{R}^D$, following [22]. The representation of pairwise encoding is then embedded into the self-attention module²,

$$Z = \text{Softmax}(QK^T + E^{(rel)} / \sqrt{D})V \quad (6)$$

²Here we only show the single-head self-attention, for multi-head self-attention, please refer to Equation 3, Equation 4 and Equation 5.

where $E_{ij}^{(rel)} = Q_i P_{ij}$, and $E^{(rel)} \in \mathbb{R}^{(m \times m \times L) \times (m \times m \times L)}$, and the E changes in each layer of the temporal transformer encoder. We further decompose the relative position embedding into height, width and temporal axes following [17], which can reduce the number of learnable parameters. We adopt the L_t -layer transformer encoder for temporal fusion, then the temporal fusion embeddings $\{x_{1,\dots,N}^{t1}, \dots, x_{1,\dots,N}^{tL}\}$ are generated.

3) *Aggregation:* In our spatial and temporal attention blocks, the class token is removed. This decision aligns with our strategy of utilizing attention for information interaction, rather than extracting frame descriptors. The sequence descriptor is aggregated by NetVLAD [6].

Given a set of D -dimensional embeddings from spatial and temporal Transformer, we combine them based on the position of patches i.e., $\{x_{1,\dots,N}^{s1} + x_{1,\dots,N}^{t1}, \dots, x_{1,\dots,N}^{sL} + x_{1,\dots,N}^{tL}\}$. Following this, we perform aggregation on the resulting $N \times L$ embeddings using NetVLAD,

$$V(k) = \sum_{i=1}^{N \times L} a_k(x_i)(x_i - c_k) \quad (7)$$

where x_i is a single embedding, c_k is the k -th centroid which is trainable parameter, and the $a_k(x_i)$ is a soft-assignment defined as:

$$a_k(x_i) = \frac{e^{w_k^T x_i + b_k}}{\sum_{k'} e^{w_{k'}^T x_i + b_{k'}}} \quad (8)$$

where w_k, b_k are also trainable parameters.

B. Loss Function

Similar to the training regime of NetVLAD, we use the max-margin triplet loss as described below:

$$\text{Loss} = \sum_k \max(\|S_a - S_p\|_2 - \|S_a - S_n^k\|_2 + \alpha, 0) \quad (9)$$

where α is the desired margin between the norm of the anchor S_a and the best positive S_p and that of S_a and

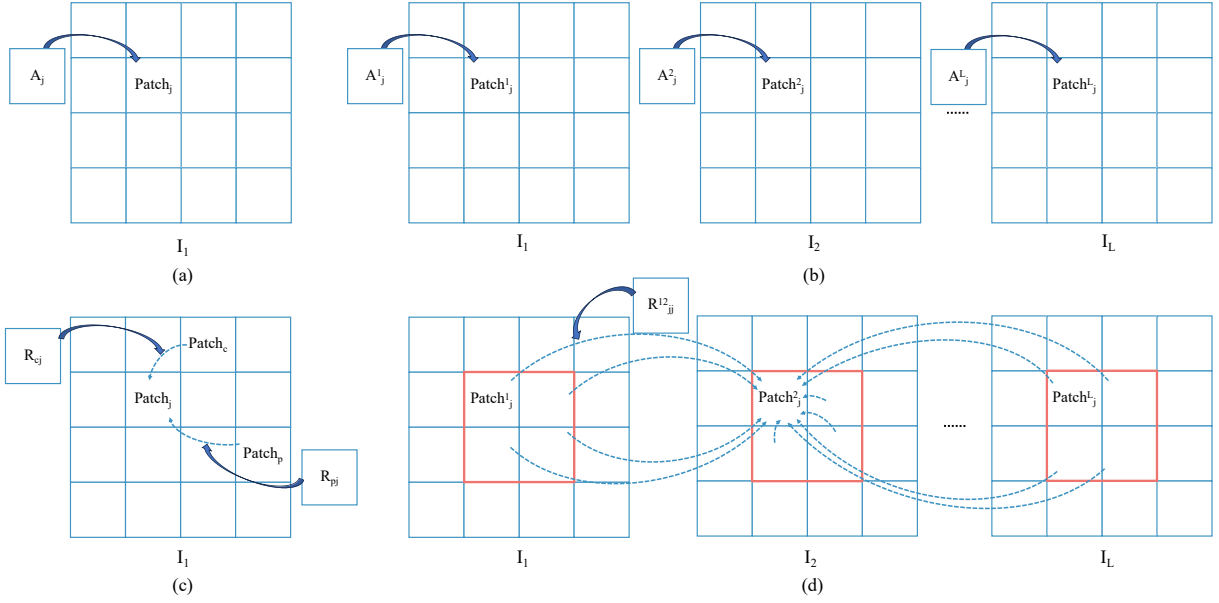


Fig. 2. **The different position embedding and sliding window.** Here we show spatial absolute position embedding (a) and relative position embedding (c), as well as temporal absolute position embedding (b) and relative position embedding (d), where we use A to represent the absolute position embedding and R for the relative position embedding. Dashed arrows indicate that information is passed between the two patches. Solid arrows indicate to fuse position embeddings to the information passing. It's important to note that absolute position embeddings are independent of the inter-patch relationships. In contrast, relative position embeddings vary based on the position relationship between patches.

TABLE I

DATASETS DETAIL. THIS TABLE SPECIFIES THE NUMBER OF IMAGES IN THE DATASET USED.

dataset		database / queries
MSLS	melbourne	101827 / 88118
	amman	953 / 835
	boston	14024 / 6724
	san francisco	6315 / 4525
	copenhagen	12601 / 6595
NordLand	train set	15000 / 15000
	test set	3000 / 3000
Oxford1	train set	2401 / 2448
	test set	1460 / 1474
Oxford2	train set	3619 / 3926
	test set	3632 / 3921

the hardest negatives S_n^k in the descriptor space, and k is the number of hard negative samples corresponding to each anchor. We train our model using a set of reference and query databases. For each query, we consider it as an anchor, its positives and negatives are generated from the reference database, which will be detailed in Section IV-B.

IV. EXPERIMENTS

A. Datasets

In our experiments, we use three datasets: MSLS [23], NordLand [24], Oxford RobotCar [25], as summarized in Table I.

1) *Mapillary Street Level Sequences (MSLS)*: Mapillary Street Level Sequences (MSLS) is a large-scale dataset for

street-level view image sequences to support large-scale VPR studies. These sequences are collected from different cities. We used Melbourne for training and Amman, Boston, San Francisco and Copenhagen for testing.

2) *NordLand*: The Nordland dataset is a collection of images of a rail journey under four seasons, covering various weather and lighting conditions. We use the Summer-Winter pair for training, and use Spring-Fall pair for testing.

3) *Oxford RobotCar*: The Oxford RobotCar dataset is a large-scale dataset for autonomous driving research. It covers different periods of road scenes. We design two experimental sub-datasets: Oxford1 splits database (2015-03-17-11-08-44, day) and query (2014-12-16-18-44-24, night) to train set and test set. Oxford2 uses database (2014-12-16-09-14-09, day) and query (2014-12-17-18-18-43, night) for train and database (2014-11-18-13-20-12, day) and query (2014-12-16-18-44-24, night) for test. These datasets are pre-processed to keep an approximate 2 meters frame separation by the latitude and longitude of each frame location.

B. Implementation Details

Architecture. We implement our method in Pytorch framework [26] with a single NVIDIA RTX A6000 card. In the patch embedding process, the CNN comprises two layers of convolution. The first layer maps 3 channels to 64 channels and the second layer maps 64 channels to 384 channels. We set the convolution parameters as follows: $kernel = 7$, $stride = 2$ and $padding = 1$. After each convolution operation, we apply the ReLU activation function followed by max pooling. Then we incorporate the spatial transformer encoder with $L_s = 4$ layers and the temporal transformer encoder with $L_t = 4$ layers. Additionally, we use a multi-head in

TABLE II
QUANTITATIVE RESULTS ON MSLS

Method	Dimension	MSLS											
		Amman			Boston			SF			Cph		
		R@1	R@5	R@10	R@1	R@5	R@10	R@1	R@5	R@10	R@1	R@5	R@10
NetVLAD [6]	4096	0.189	0.251	0.277	0.179	0.238	0.267	0.289	0.398	0.455	0.405	0.534	0.594
NetVLAD+SeqMatch [11]	4096	0.246	0.302	0.330	0.204	0.239	0.257	0.363	0.430	0.460	0.504	0.612	0.657
SeqNet [11]	4096	0.269	0.376	0.408	0.274	0.354	0.390	0.556	0.671	0.728	0.462	0.581	0.637
SeqVLAD [12]	24576	0.300	0.448	<u>0.519</u>	0.466	0.628	0.678	0.661	0.826	<u>0.863</u>	0.564	0.722	0.777
Ours	24576	<u>0.303</u>	0.423	0.511	0.504	0.645	<u>0.688</u>	0.680	0.841	0.864	0.608	0.765	0.801
SeqVLAD w/ PCA	4096	0.294	<u>0.442</u>	0.526	0.465	0.623	0.675	0.656	0.822	0.859	0.560	0.720	0.774
Ours w/ PCA	4096	0.306	0.411	0.510	<u>0.502</u>	0.645	0.691	<u>0.671</u>	<u>0.839</u>	0.860	<u>0.604</u>	<u>0.760</u>	0.801

The best and second-best results for each dataset are highlighted. The best overall results on each dataset are indicated in **bold**, while the second-best results are underlined.

TABLE III
QUANTITATIVE RESULTS ON NORDLAND AND OXFORD ROBOTCAR

Method	Dimension	NordLand			Oxford1			Oxford2		
		R@1	R@5	R@10	R@1	R@5	R@10	R@1	R@5	R@10
NetVLAD [6]	4096	0.377	0.543	0.615	0.468	0.696	0.779	-	-	-
NetVLAD+SeqMatch [11]	4096	0.610	0.705	0.746	0.672	0.784	0.846	-	-	-
SeqNet [11]	4096	0.797	0.905	0.930	0.741	0.875	0.933	-	-	-
SeqVLAD [12]	24576	0.964	0.992	0.993	<u>0.966</u>	<u>0.982</u>	<u>0.989</u>	0.844	0.929	0.958
Ours	24576	0.971	0.995	0.995	0.958	0.978	0.988	0.868	<u>0.944</u>	<u>0.968</u>
SeqVLAD w/ PCA	4096	0.963	0.991	0.994	0.967	0.982	0.990	0.847	0.932	0.961
Ours w/ PCA	4096	0.971	0.995	0.995	0.955	0.977	0.986	<u>0.866</u>	0.945	0.969

The best and second-best results for each dataset are highlighted. The best overall results on each dataset are indicated in **bold**, while the second-best results are underlined.

transformer with $h = 6$ heads. In the temporal transformer encoder, we set the size of sliding window $m = 6$ and the $stride = 3$. Both the inputs and outputs of the transformers are embeddings with a dimensionality of $D = 384$. Inside the NetVLAD module, we configure the number of clusters to be 64, yielding sequence descriptors with dimensions of 384×64 without the application of Principal Component Analysis (PCA) [27]. To facilitate comparison with other methods, we perform dimensionality reduction using PCA, reducing the dimensionality to 4096.

Training. In the training phase, we initialize the model with pre-trained parameters from CCT [21] and adopt the Adam optimizer [28]. All images are resized to 384×384 . The learning rate is configured as 0.0001, 0.001 and 0.0001 for spatial transformer encoder, temporal transformer encoder and NetVLAD respectively. We set the $batchsize = 4$, with each batch consisting of a query sequence, a best positive sequence and 5 hardest negative sequences ($k = 5$ as referenced in Equation 9). The length of each sequence is set to $L = 5$. We specify the margin in triplet loss as $\alpha = 0.1$. The mining method [6] is used to select samples, i.e., we initially select samples by GNSS labels between the query and the database, and then we select the best positive and the hardest negatives by cosine distance in the descriptor space. Since selecting negatives from the whole dataset is time and space consuming, we adopt partial mining [23]. Namely we randomly sample a subset of negatives

by GNSS labels filtering, and we use a cache to store the descriptors of sub-negatives. The cache is employed for selecting negatives by cosine distance for triplet samples, and it is refreshed after every 1000 iterations. We implemented early stopping by halting the training if the Recall@5 does not show improvement for five consecutive epochs. We set the positive distance threshold to 10 meters and the negative distance threshold to 25 meters.

Evaluation. In the evaluation phase, we use Recall@K as the performance metric. Recall@K is defined as the ratio of the number of correct queries retrieved to the total number of queries. A correct retrieval is defined as at least one of the top K retrieval is within the given localization radius from the ground truth position of the query. We use a localization radius of 10 meters, 20 meters and 1 frame respectively for Oxford, MSLS and Nordland datasets.

C. Results

1) **Comparison with the State-of-the-art Methods:** The chosen baseline methods include the state-of-the-art methods using sequence descriptors, i.e., SeqNet [11] and SeqVLAD [12]. Additionally we also compare with NetVLAD [6] and NetVLAD+SeqMatch [11]. For a fair comparison, all the experimental results are reproduced via our setting in Section IV-A and Section IV-B.

Table II and Table III show our method results in comparison to the baseline methods on MSLS, NordLand and Oxford RobotCar. From the quantitative results, it reveals

that NetVLAD performs worse than other methods. This suggests that sequence VPR significantly outperforms the single-frame VPR. In addition, the methods based on sequence descriptors outperforms the method based on SeqMatch.

Compared to SeqNet, our method outperforms it across all datasets. We observe a Recall@1 improvement of over 10% in most datasets, except a 4% improvement in Amman. SeqNet generates a sequence descriptor through a weighted sum of frame descriptors. These frame descriptors are created by aggregating the local features of each frame. While local features can be discriminative for individual frames within a sequence, they may not exhibit the same level of discriminative power across all sequences. In contrast, our method directly derives the sequence descriptors from the local features of all frames within a sequence. This approach ensures that our descriptor maintains its discriminative qualities across different sequences.

Additionally, compared with SeqVLAD, our method exhibits superior performance in most datasets, except Amman and Oxford1. Notably, SeqVLAD does not take into account the temporal correlation or change across multiple frames. As shown in Figure 6 (a)(c), the SeqVLAD is susceptible to dynamic objects, e.g., bicyclists, and is sensitive to illumination changes from day to night or variations in weather conditions. Conversely, our proposed cross-frames temporal attention can effectively capture local regions correspondences to learn patterns that persist over time. This property renders our sequence descriptors more robust to illumination changes and local scene variations across sequence. Figure 3 provides further insight by illustrating the attention mechanisms of both our method and SeqVLAD for different regions within query sequences from Figure 6 (a)(c), substantiating the aforementioned conclusions. While our method’s performance in Oxford1 is slightly lower than SeqVLAD, there is a noteworthy improvement of over 2% for Recall@1. Oxford1 has a smaller training set compared to Oxford2, but our model has a higher parameter count than SeqVLAD, making it more challenging to train effectively. On the other hand, SeqVLAD tends to be more susceptible to overfitting.

Finally, we delve into the impact of reducing the dimensionality of sequence descriptors. Our research reveals that when descriptors undergo dimensionality reduction via Principal Component Analysis (PCA) into a 4096-Dimensional space, their performance remains on par with that of the full-sized descriptors.

2) *Ablation Studies:* We conduct ablation studies on the four test cities of MSLS to analyze the effectiveness of the *spatio-temporal attention with position embedding* and the *sliding window setting*. As shown in Figure 4, we compare the experimental results of spatio-temporal attention with position embedding. It can be clearly observed that descriptors extracted via spatial attention achieve better performance than those extracted by temporal attention. This may indicate that the spatial structure plays a dominant role in the extraction process of sequence descriptors. But our sequence descriptors extracted via spatio-temporal attention

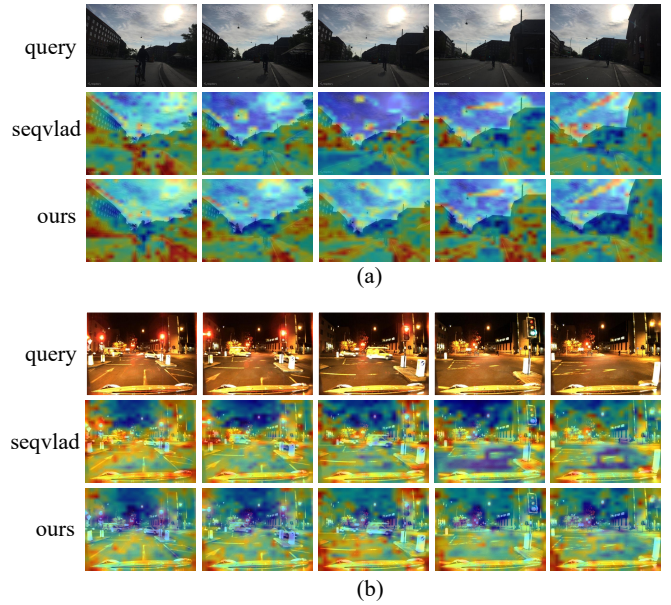


Fig. 3. **Visualizations on attention.** Here are attentions of our method and SeqVLAD for different regions of the query sequences which is in Figure 6 (a)(c). Red portions indicate more focus, and blue portions indicate less focus. Compared to SeqVLAD, our method focuses less on dynamic objects and more on road elements.

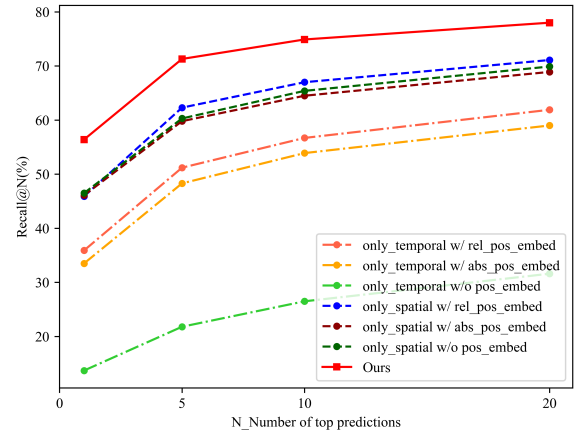


Fig. 4. **Ablation Studies for spatio-temporal effectiveness and position embedding.** We show the comparison of Recall@N performances with only spatial or temporal module, and two kinds of position embedding or w/o position information. In addition, the position embedding is trained from scratch without pre-trained parameters.

achieve the best performance. This suggests that fusing temporal information to spatial structure can further improve the representation of the descriptors.

Furthermore, the role of position embedding is slight for spatial attention. However, for temporal attention, the position embedding is crucial. Fusing position information can greatly improve performance of descriptors, and relative position embedding is superior to absolute position embedding.

In addition, we explore how the setting of the sliding window affects the ability to capture the dynamics of local features in temporal attention. We compare different sliding

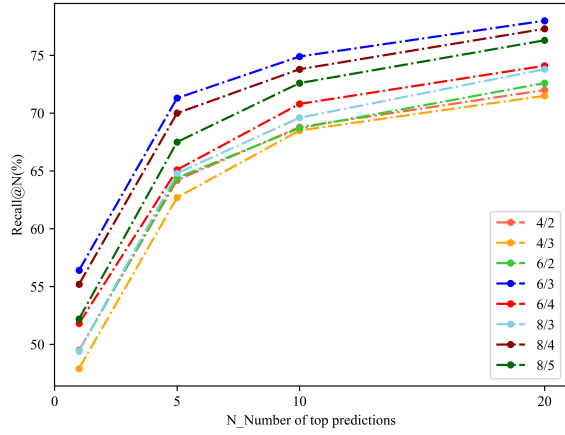


Fig. 5. **Ablation Studies for sliding window settings.** We show the comparison of Recall@N performances with different sliding window settings, where m/s demonstrates the size and stride of the sliding window respectively.

TABLE IV

RESOURCE CONSUMPTION AND MODEL SIZE. THE MS/FRA INDICATES THE TIME OF EXTRACTING A FRAME DESCRIPTOR, AND MS/SEQ INDICATE THE TIME OF EXTRACTING A SEQUENCE DESCRIPTOR.

Method	Extraction latency	GPU Memory	GFLOPs	Params
NetVLAD [6]	8.8 ms/fra	57.26 MB	45.12	14.74 M
SeqNet [11]	6.2 ms/seq	320.01 MB	0.84	83.89 M
SeqVLAD [12]	8.9 ms/seq	59.88 MB	32.71	7.15 M
Ours	18.7 ms/seq	103.74 MB	63.74	13.06 M

window settings, where 4×4 , 6×6 and 8×8 are set for the size of window, and $\{2, 3\}$, $\{2, 3, 4\}$ and $\{3, 4, 5\}$ are set for the stride respectively.

As can be observed from the Figure 5, for the same stride, a larger sliding window performs better than a smaller one, but beyond a certain size, the performance decreases. Finally, the optimal value of stride is half of the sliding window size.

3) **Runtime Analysis and Memory Footprint:** In real-world VPR systems, it is crucial to take into account factors like latency and scalability. Table IV provides insights into the computational time, GPU memory requirements and model size of the compared techniques in evaluation. The reason that SeqNet extracts sequence descriptors more swiftly and with lower GFLOPs is the NetVLAD descriptors for each image have been pre-extracted offline and stored on disk, otherwise the time taken by NetVLAD to extract the descriptors of images would need to be taken into account. In addition, the memory footprint and model parameters of SeqNet are influenced by both the descriptor dimension and sequence length, which are proportional to $D \times D \times L$, where D represents the descriptor dimension and L represents the sequence length. In contrast, our approach and SeqVLAD extract sequence descriptors directly from the original image sequences, with the entire process being executed online. Additionally, our model considers the interaction among

consecutive frames, making it more intricate than SeqVLAD. Consequently, it takes more time to extract a sequence descriptor.

4) **Qualitative Results:** In Figure 6, we show our retrieval sequence compared with SeqNet and SeqVLAD retrieval Sequences in MSLS street view and highway, Oxford and NordLand.

Sequences marked with green and red borders imply correct and incorrect retrievals, respectively. Sequences marked with orange borders denote that the retrieval sequence and the query have the same view, but their GNSS labels define that they are not the same “place”. Based on the qualitative results, our method demonstrates the capability to handle changes in lighting condition caused by day-night transitions and weather changes. In addition, it is less susceptible to dynamic occlusions and partial scene changes, such as pedestrians and vehicles on the road and changes due to road maintenance.

V. CONCLUSION

VPR holds immense potential for various applications. Our work aims to provide a new perspective on sequence-based VPR. Instead of merely aggregating multiple frames spatially, we introduce the fusion of features in the temporal dimension. We use a spatio-temporal attention approach to provide a discriminative descriptor of sequences with improved accuracy compared with existing methods. Additionally, our findings emphasize the significance of both spatial structure and temporal variation for sequence descriptors. We anticipate that these novel insights will serve as a solid foundation for improved utilization of sequence information in future research endeavors.

REFERENCES

- [1] S. Lowry, N. Sünderhauf, P. Newman, J. J. Leonard, D. Cox, P. Corke, and M. J. Milford, “Visual place recognition: A survey,” *IEEE transactions on robotics*, vol. 32, no. 1, pp. 1–19, 2015.
- [2] H. Jégou, M. Douze, C. Schmid, and P. Pérez, “Aggregating local descriptors into a compact image representation,” in *2010 IEEE Computer Society Conference on Computer Vision and Pattern Recognition*, 2010, pp. 3304–3311.
- [3] J. Sánchez, F. Perronnin, T. Mensink, and J. Verbeek, “Image classification with the fisher vector: Theory and practice,” *International journal of computer vision*, vol. 105, no. 3, pp. 222–245, 2013.
- [4] H. Jégou, F. Perronnin, M. Douze, J. Sánchez, P. Pérez, and C. Schmid, “Aggregating local image descriptors into compact codes,” *IEEE transactions on pattern analysis and machine intelligence*, vol. 34, no. 9, pp. 1704–1716, 2011.
- [5] Z. Chen, O. Lam, A. Jacobson, and M. Milford, “Convolutional neural network-based place recognition,” *arXiv preprint arXiv:1411.1509*, 2014.
- [6] R. Arandjelovic, P. Gronat, A. Torii, T. Pajdla, and J. Sivic, “Netvlad: Cnn architecture for weakly supervised place recognition,” in *Proceedings of the IEEE conference on computer vision and pattern recognition*, 2016, pp. 5297–5307.
- [7] H. Jin Kim, E. Dunn, and J.-M. Frahm, “Learned contextual feature reweighting for image geo-localization,” in *Proceedings of the IEEE Conference on Computer Vision and Pattern Recognition*, 2017, pp. 2136–2145.
- [8] M. J. Milford and G. F. Wyeth, “Seqslam: Visual route-based navigation for sunny summer days and stormy winter nights,” in *2012 IEEE international conference on robotics and automation*. IEEE, 2012, pp. 1643–1649.

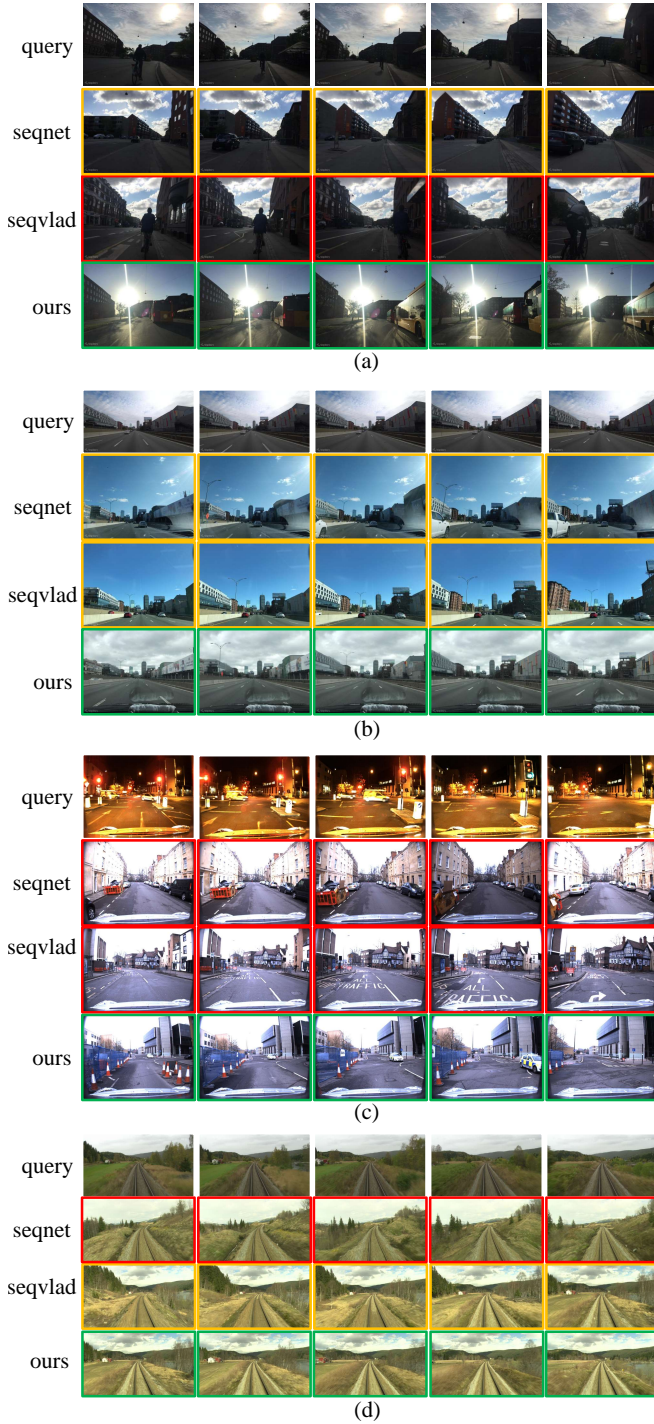


Fig. 6. **Qualitative results.** In these examples, the proposed method successfully retrieves the matching reference sequence in MSLS street (a) view and highway (b), Oxford (c) and NordLand (d), while SeqNet and SeqVLAD produce incorrect place matches. Green and red indicate correct and incorrect retrievals, respectively. While orange indicates the same view but beyond a certain GNSS label threshold, which is also defined as incorrect retrievals.

- [9] S. M. Siam and H. Zhang, "Fast-seqslam: A fast appearance based place recognition algorithm," in *2017 IEEE International Conference on Robotics and Automation (ICRA)*. IEEE, 2017, pp. 5702–5708.
- [10] J. M. Facil, D. Olid, L. Montesano, and J. Civera, "Condition-invariant multi-view place recognition," *arXiv preprint arXiv:1902.09516*, 2019.
- [11] S. Garg and M. Milford, "Seqnet: Learning descriptors for sequence-based hierarchical place recognition," *IEEE Robotics and Automation Letters*, vol. 6, no. 3, pp. 4305–4312, 2021.
- [12] R. Mereu, G. Trivigno, G. Berton, C. Masone, and B. Caputo, "Learning sequential descriptors for sequence-based visual place recognition," *IEEE Robotics and Automation Letters*, vol. 7, no. 4, pp. 10 383–10 390, 2022.
- [13] F. Lu, B. Chen, Z. Guo, and X. Zhou, "Visual sequence place recognition with improved dynamic time warping," in *2019 IEEE 31st International Conference on Tools with Artificial Intelligence (ICTAI)*. IEEE, 2019, pp. 1034–1041.
- [14] C. Feichtenhofer, A. Pinz, and R. P. Wildes, "Spatiotemporal multiplier networks for video action recognition," in *Proceedings of the IEEE conference on computer vision and pattern recognition*, 2017, pp. 4768–4777.
- [15] J. Li, X. Liu, W. Zhang, M. Zhang, J. Song, and N. Sebe, "Spatio-temporal attention networks for action recognition and detection," *IEEE Transactions on Multimedia*, vol. 22, no. 11, pp. 2990–3001, 2020.
- [16] G. Bertasius, H. Wang, and L. Torresani, "Is space-time attention all you need for video understanding?" in *ICML*, vol. 2, no. 3, 2021, p. 4.
- [17] Y. Li, C.-Y. Wu, H. Fan, K. Mangalam, B. Xiong, J. Malik, and C. Feichtenhofer, "Mvitv2: Improved multiscale vision transformers for classification and detection," in *Proceedings of the IEEE/CVF Conference on Computer Vision and Pattern Recognition*, 2022, pp. 4804–4814.
- [18] J. Ji, C. Xu, X. Zhang, B. Wang, and X. Song, "Spatio-temporal memory attention for image captioning," *IEEE Transactions on Image Processing*, vol. 29, pp. 7615–7628, 2020.
- [19] A. Aich, M. Zheng, S. Karanam, T. Chen, A. K. Roy-Chowdhury, and Z. Wu, "Spatio-temporal representation factorization for video-based person re-identification," in *Proceedings of the IEEE/CVF international conference on computer vision*, 2021, pp. 152–162.
- [20] A. Dosovitskiy, L. Beyer, A. Kolesnikov, D. Weissenborn, X. Zhai, T. Unterthiner, M. Dehghani, M. Minderer, G. Heigold, S. Gelly, J. Uszkoreit, and N. Houlsby, "An image is worth 16x16 words: Transformers for image recognition at scale," in *International Conference on Learning Representations*, 2021.
- [21] A. Hassani, S. Walton, N. Shah, A. Abuduweili, J. Li, and H. Shi, "Escaping the big data paradigm with compact transformers," *arXiv preprint arXiv:2104.05704*, 2021.
- [22] P. Shaw, J. Uszkoreit, and A. Vaswani, "Self-attention with relative position representations," *arXiv preprint arXiv:1803.02155*, 2018.
- [23] F. Warburg, S. Hauberg, M. Lopez-Antequera, P. Gargallo, Y. Kuang, and J. Civera, "Mapillary street-level sequences: A dataset for lifelong place recognition," in *Proceedings of the IEEE/CVF conference on computer vision and pattern recognition*, 2020, pp. 2626–2635.
- [24] N. Sünderhauf, P. Neubert, and P. Protzel, "Are we there yet? challenging seqslam on a 3000 km journey across all four seasons," in *Proc. of workshop on long-term autonomy, IEEE international conference on robotics and automation (ICRA)*, 2013, p. 2013.
- [25] W. Maddern, G. Pascoe, C. Linegar, and P. Newman, "1 year, 1000 km: The oxford robotcar dataset," *The International Journal of Robotics Research*, vol. 36, no. 1, pp. 3–15, 2017.
- [26] A. Paszke, S. Gross, F. Massa, A. Lerer, J. Bradbury, G. Chanan, T. Killeen, Z. Lin, N. Gimelshein, L. Antiga *et al.*, "Pytorch: An imperative style, high-performance deep learning library," *Advances in neural information processing systems*, vol. 32, 2019.
- [27] H. Jégou and O. Chum, "Negative evidences and co-occurrences in image retrieval: The benefit of pca and whitening," in *Computer Vision—ECCV 2012: 12th European Conference on Computer Vision, Florence, Italy, October 7-13, 2012, Proceedings, Part II 12*. Springer, 2012, pp. 774–787.
- [28] D. P. Kingma and J. Ba, "Adam: a method for stochastic optimization," in *International Conference on Learning Representations*, 2015.